ION BEAM ANALYSIS METHODS FOR DETERMINING MAJOR AND MINOR ELEMENT CONCENTRATIONS IN ARTEFACTS*

HANS HENRIK ANDERSEN[1] and HARRY J. WHITLOW[2, 3]

[1] Physics Laboratory II, H.C. Ørsted Institute,
Universitetsparken 5, DK-2100 Copenhagen Ø
[2] University of Helsinki, Accelerator Laboratory
Hämeentie 100, SF-00550 Helsinki
[3] Present address: Tandem Accelerator Laboratory,
University of Uppsala, Box 533, S-751 21 Uppsala

Abstract

Two quantitative analytical techniques, Rutherford Backscattering Spectrometry (RBS) and Proton Induced X-ray Emission (PIXE), based on MeV ion beams from a Van de Graaff accelerator have been used in an archaeometric determination of major and minor element concentrations in patinated flint artefacts and a metal fragment found during excavation of a viking settlement.

A red/brown patination on an artefact surface that had developed subsequent to exposure by flaking 6200 years ago was demonstrated to be associated with a significantly higher Fe concentration at the surface compared to the bulk and further this Fe was concentrated in the micro-fissures along the grain boundaries through which ground water percolates into the flint.

Another type of patination, brown and purple/red spots or so-called seaweed spots, on flint artefacts that had been excavated from a site that had been flooded by sea were found to be associated with high concentrations of manganese and in the case of a modern sample from which seaweed had been removed, also iodine. Although this does not confirm that seaweed spots are actually due to seaweed the result suggests they are due to the action of marine organisms.

The composition of a metal fragment, that was found during excavation of a viking-age settlement, and suspected of having been soldered was determined to be chiefly Fe with minor components Sn and Pb. The Pb/Sn concentration ratio of about 2 at.% corresponds to an alloy like modern tinplate which suggests the specimen might be of modern origin.

Introduction

Ion accelerators that produce ions of 0.5—10 MeV energy are finding increasing application for ion-beam analysis of the elemental and isotopic composition of samples in almost all branches of science and technology from medicine to cosmology. A significant application of ion beam analysis in archaeometry is accelerator mass-spectrometry for dating purposes. Other ion-beam analytical techniques, based on detection of ion bombardment induced radiation (x-, γ-rays) or backscattered ions from the object under investigation, can provide a wide range of quantitative archaeometric information. In contrast to neutron activation and x-ray fluorescence which are bulk analysis techniques, ion beam analysis techniques are surface specific, i.e. they detect closer to

---

the surface than a few μm. We have employed two of these techniques, Proton Induced x-ray Emission (PIXE) and Rutherford Backscattering Spectrometry (RBS) to determine major and minor elemental compositions and their spatial distributions within artefacts.

The particular archaeometric problems we have addressed are:

(i)   The origin of a brown-red patina that formed on a flint surface subsequent to its exposure 6200 years B.P.

(ii) The cause of so-called seaweed-spot patination.

(iii) The composition of a ferrous metal fragment found during excavation of a viking age settlement and determination whether its proposed restoration technique gave rise to loss of minor components due to leaching.

2.   Techniques

2.1 *Proton Induced x-ray Emission (PIXE)*

Briefly the principles of PIXE, which are discussed in detail in a number of reviews (Folkmann, 1975; Johansson and Johansson, 1976; Kahn and Crumpton, 1981) are as follows: a beam of protons of 1—4 MeV energy from an accelerator is directed at the target whose composition is to be analysed (Fig. 1). After passing through the surface of the target the protons lose energy chiefly by excitation and ionization of the atoms in the target (so-called electronic stopping). This excitation leads to target atoms with vacancies in the inner electron shell which subsequently capture electrons from the continuum and outer shells and emit x-ray photons of characteristic energy or Auger electrons. The x-rays are detected in the energy-dispersive Si:Li detector (Fig. 1) or a crystal spectrometer and the resulting pulses are sorted in a multi-channel analyser to produce an x-ray energy spectrum. The size of the peaks in the pixe spectrum corresponding to the characteristic x-ray energies for each element reflects indirectly that element's concentration in the target.
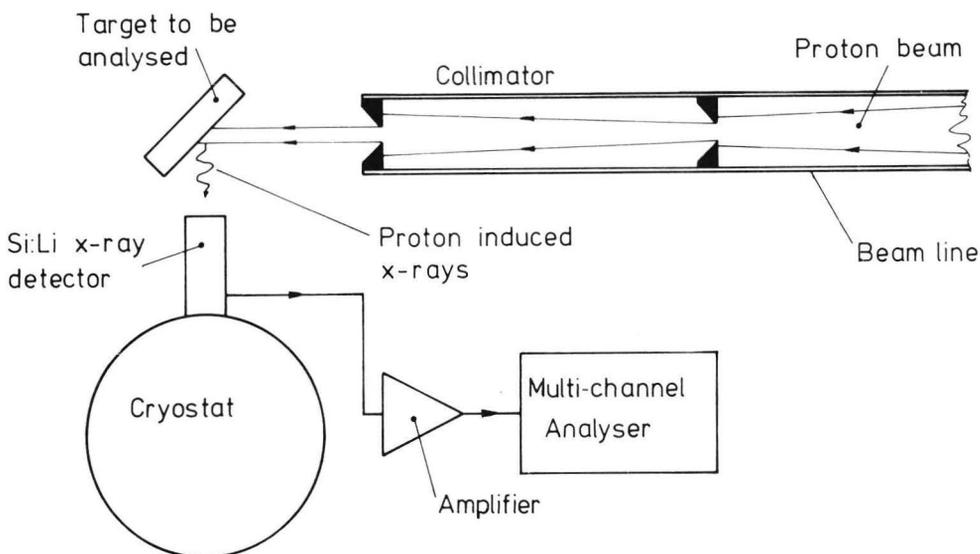

Fig. 1. Set-up for Proton Induced X-ray Emission (PIXE) measurements. The measurements can be carried out either in vacuum or in atmosphere. In the latter case the proton beam passes out from the vacuum of the beam line into atmosphere via a thin vacuum-tight window.

The PIXE technique is characterized by:

(i) Good sensitivity for elements with atomic number Z > 20. (If PIXE is combined with Proton Induced Gamma Emission (PIGE) virtually all elements may be detected with good sensitivity (Hänninen et al., 1980; Hyvönen—Dabek, 1981; Räisänen, 1984)).

(ii) Sensitivity down to a depth of 5—10 μm. The lateral resolution is determined by the proton beam dimensions (typically 1 mm^2.)

(iii) The possibility of conducting the analysis in air rather than vacuum through the use of external beam techniques. (Chen 1980, 1981; Kahn and Crumpton, 1981; Johnsson, 1976; Folkmann, 1975; Baijot-Stroobands and Bodart F., 1977.) This is a feature of importance for archaeometric application where the artefact in question often cannot tolerate exposure to vacuum.

PIXE has been used with considerable success in archaeometric studies of ancient metals (Ahlberg, 1976; J. Cheng, 1980; Duerden et al., 1980; Demortier, 1982), Pottery (Baijot-Stroobands, 1977; Duerden, 1980) and for provenancing chert and obsidian (Duerden et al., 1980; Ambrose et al., 1981).

2.2 Rutherford Backscattering Spectrometry (RBS)

The basis of the RBS technique is illustrated in Fig. 2. (for a detailed description the reader is referred to the monograph by Chu, Mayer and Nicolet (1978)). The bombarding ions which are usually helium ions of 0.5—5 MeV energy are collimated to a parallel beam that impinges on the target which is to be analysed. A small fraction of the ions that penetrate the surface are subsequently backscattered out of the target in a single large angle collision with the nucleus of a target atom — so called Rutherford backscattering. (The vast majority of ions penetrate the target without undergoing such large-angle scattering.) The backscattered ions are detected by a charged particle detector shielded so that it only sees ions that have been scattered through a fixed scattering angle (Fig. 2 a, b). A multi-channel analyser is employed to sort the pulses to produce a backscattered particle energy spectrum. The energy is determined by (a) the energy loss due to stopping during its passage through the target and (b) the kinematics of scattering. For the geometry of Fig. 2, (a) is linearly related through the stopping power to the depth at which scattering takes place. Whilst (b) is a constant fraction of the projectile ion energy immediatly prior to scattering. The fraction for a given ion species and a fixed scattering angle as in Fig. 2 is determined by the mass of the target atom from which scattering occurred; the heavier the scattering atom, the higher the backscattered energy. Thus the contribution to the backscattering spectrum at some energy for some constituent element of the target is proportional to the concentration of that element at the depth corresponding to backscattering at the energy in question. Thus as illustrated in Fig. 2 (b—c), the RBS spectrum is a superposition of the concentration profiles of the constituent elements in the target. The profiles are staggered along the energy axis according to the kinematic factors. Typically the attainable depth resolution for archaeological specimens is 200—1000 Å with a mass resolution of 1 a.m.u. at mass 28 and 25 a.m.u. at mass 200. The depths over which concentration profiling may be obtained is typically 0.1—1 μm. This is about one tenth of the depth analysed by PIXE. The sensitivities which are better for higher Z elements lie in the 10—1000 p.p.m. range. The lateral resolution is, as for PIXE determined by the dimensions of the ion beam which is typically 1 mm^2.
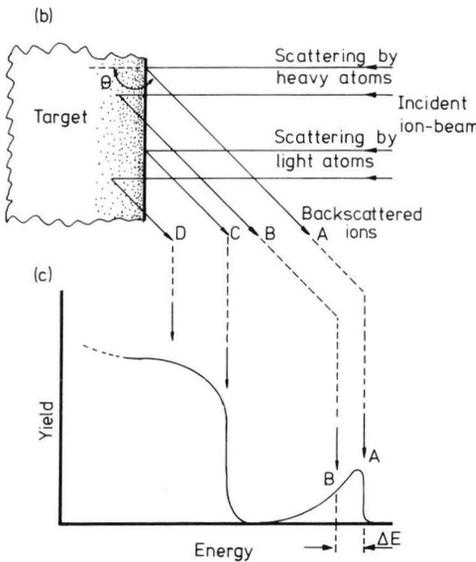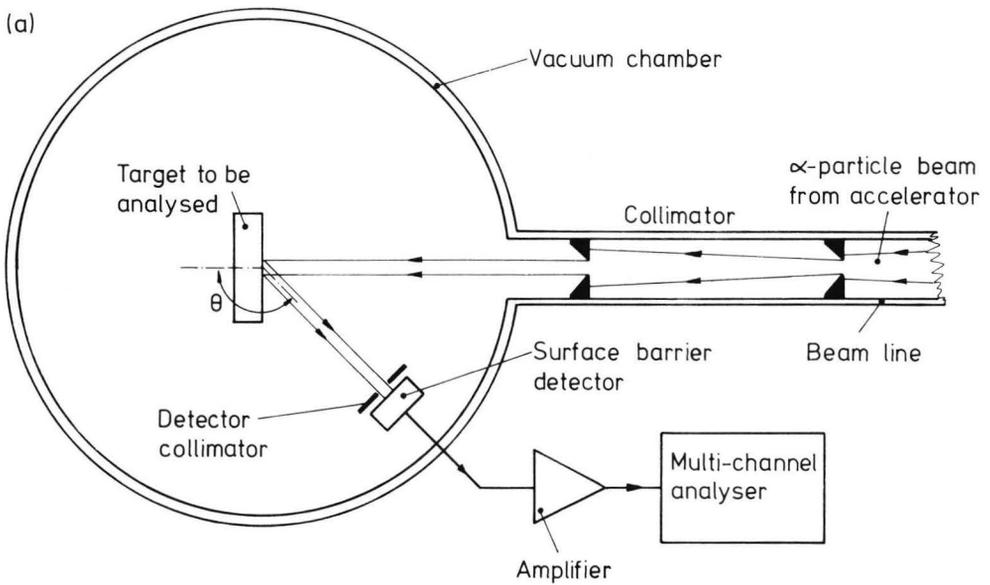
(a)

(b)

(c)

Fig. 2. Principles of the Rutherford Backscattering Spectrometry (RBS) technique.
(a) Target chamber set-up for RBS analysis.
(b) Relation between ion trajectory in the target and backscattered particle energy. The depth distribution of a heavy minor element X in the light target Y is represented by the density of dark points.
(c) Backscattered particle energy spectrum from (b).

A corresponds to ions backscattered from X atoms at the surface, because of the higher mass of X these are backscattered with the highest energies. B corresponds to ions backscattered from X at some depth in the target. The energy difference ΔE is linearly related to the depth at which scattering took place. C corresponds to ions backscattered from Y at the surface. These have lower energy than A due to the mass of Y being lower than X. D corresponds to ions backscattered from Y some depth below the surface. Note the backscattering yield from X v.s. energy reflects its depth distribution in the target.

3. Experimental investigations

3.1 Brown patination of Flint

Patination is a term used to describe the colouration of minerals due to chemical alteration by the environment. Patina on flint can take a number of forms (Rottländer 1975, 1976). Here we are concerned with the brown patination. Most often this has been tacitly assumed to be due to iron, however with Electron Probe Micro-Analysis (EPMA) Rottländer (1975) found no difference in the iron content of the surface and interior of a brown-patinated sample. In contrast, Secondary Ion Mas Spectroscopy
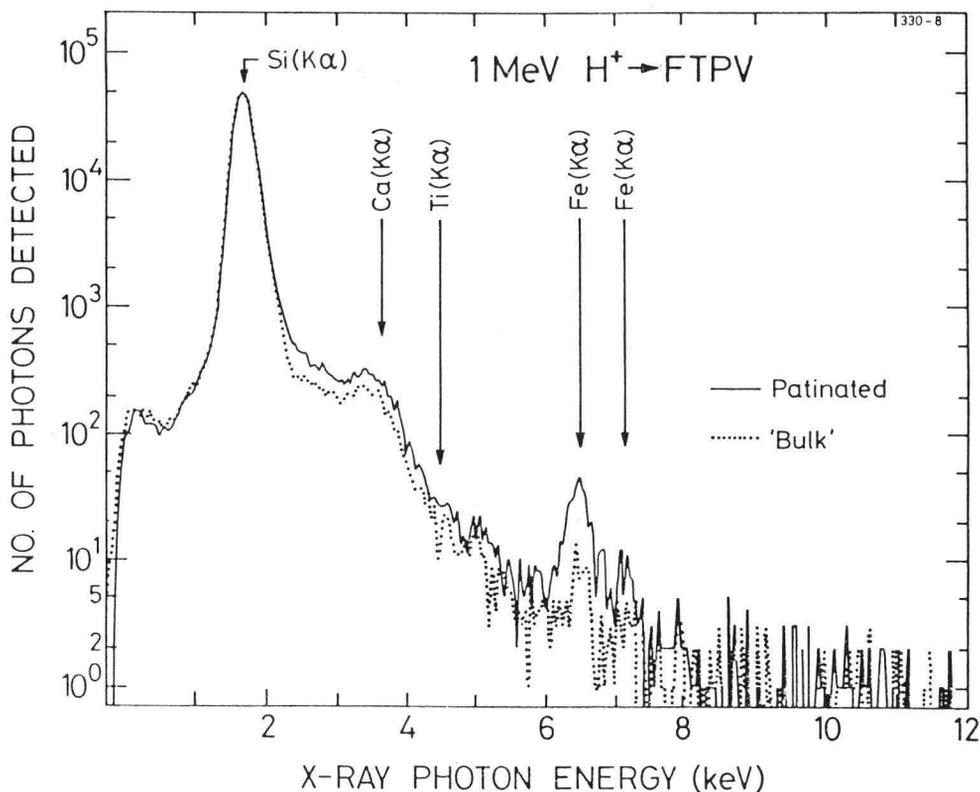
Fig. 3. PIXE spectrum from patinated and fracture-exposed bulk surface of 1592 FTPV. The red patination is seen to stem from an enhanced iron concentration.

(SIMS) (Hofer 1974) showed the patinated surface of one of our samples had an iron concentration that was enhanced relative to the bulk.

We have investigated a sample (1592 FTPV) from a mesolithic site, Ringkloster near Skanderborg, Denmark (S.H. Andersen 1975). Prehistoric working of this sample, a flint core, exposed the surface on which a brown patination subsequently formed. The thickness of the patina extends to about 0.8 mm depth. A corresponding ^{14}C dating result (K-1765) is 5530 yrs which may be calibrated to give a date for exposure of the surface of 6200 B.P. 1592 FTPV was found at a depth of 20 cm below the surface of a meadow that was periodically swamped but never water-logged for an extended period. 1592 FTPV was fractured to yield samples of freshly exposed surfaces to supplement the patinated ones. The surfaces were covered with 500 Å thick metal layers to render the surface electrically conducting.

PIXE analysis was conducted with 1 MeV protons from the University of Aarhus 2 MV Van de Graaff accelerator and an energy-dispersive Si:Li X-ray detector. In Figure 3 a comparison of the PIXE spectra from the bulk and patinated surfaces of 1592 FTPV is presented. A qualitative evaluation of these spectra shows that within 10 μm of the surface the iron concentration is about 7 times greater for the patinated surface than that of the bulk-fracture surface. Apart from silicon, prominent peaks are seen that stem from Al, Ca and Fe. Unfortunately pile-up from the intense Si Kα peak blurred some of the features in which we are interested. Less prominent peaks seen
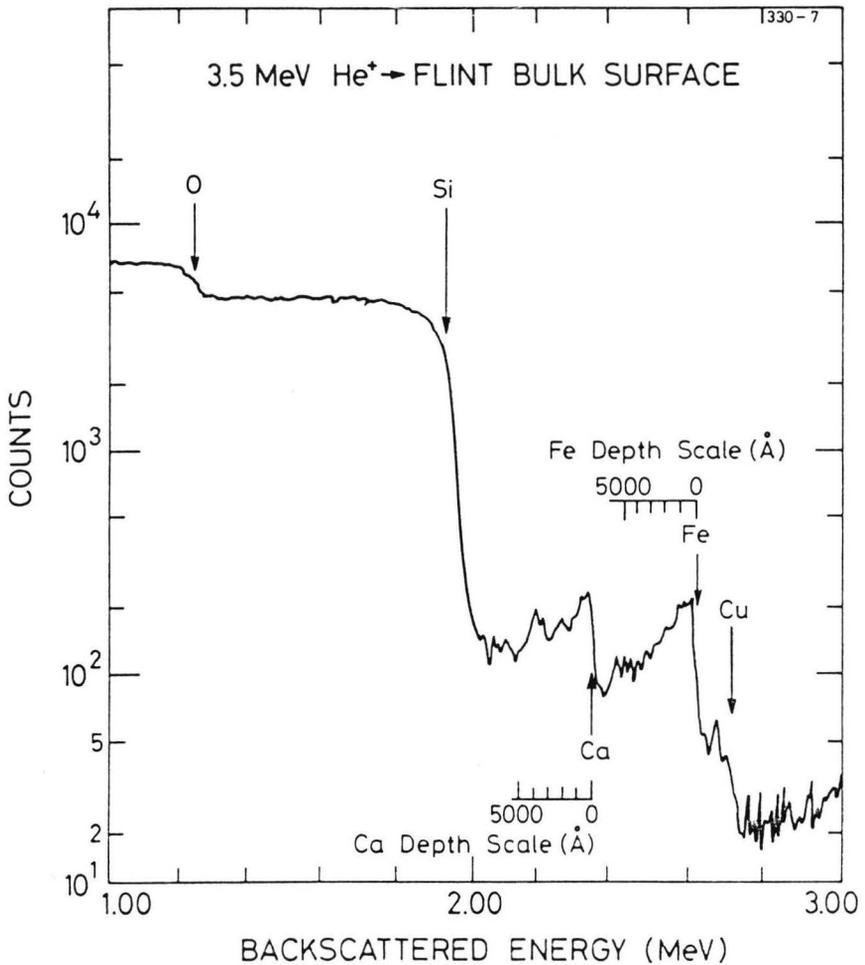
Fig. 4. RBS spectrum of fracture-exposed bulk surface of 1592 FTPV. Note the enhanced Fe concentration at depths less than 4000 Å.

when the Si Kα peak was filtered out by an absorber, stem from P, K, Ti, Mn and Ca. The Al Kα peak stems from the 500 Å conducting metal layer whilst the potassium and phosphorus may stem from the presence of fertilizer deposited in the flint from the ground water.

RBS measurements were carried out using 3.5 MeV He⁺ ions from a 4.75 MV van de Graaff accelerator at the University of Aarhus. Fig. 4 shows the RBS spectra from the bulk-fracture surface of 1592-FTPV. This shows the perhaps surprising result that within 0.4 μm of the fracture-exposed bulk surface the Fe and Ca concentrations are enhanced. We note the region over which Ca and Fe is enhanced is so thin that no enhancement would be detected by PIXE.

According to Micheelsen (1966) who studied dark flint from Stevns Klint, Denmark, flint consists of polycrystalline α-quartz with chalk inclusions. The α-quartz grains have sizes of some 20—30 μm and are divided into subgrains of 0.2—3 μm by low-angle boundaries. The α-quartz grains are bound together by OH bonds. Nuclear resonance profiling studies of water uptake in flint reported by us previously (Andersen, 1981,
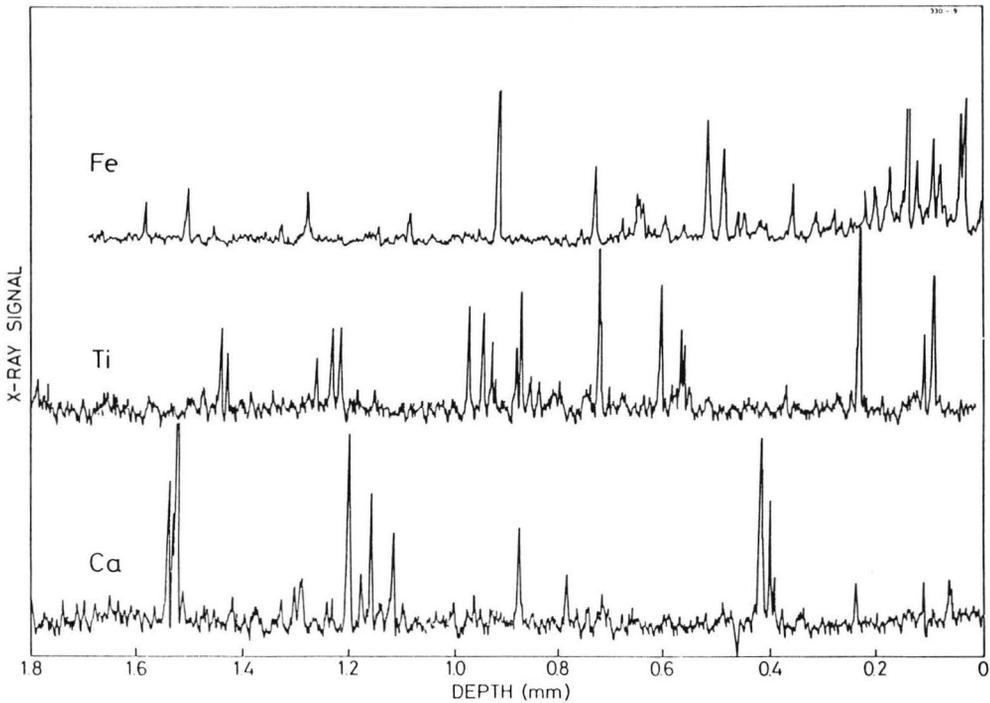
Fig. 5. Electron Probe MicroAnalysis (EPMA) scan of a 1 μm slab of 1592 FTPV cut perpendicular to the surface.

Andersen and Whitlow 1984) show that water is efficiently transported into flint along the intergranular micropores and fissures over a time scale of a few days. Further it was concluded that flint preferentially fractures inter-granually along the water containing grain boundary fissures rather than intra-granually — a conclusion in agreement with Olausson's and Larsson's (1981, 1982) Scanning Electron Microscope (SEM) study of flint fracture. Thus we interpret the near-surface enhancement of Ca and Fe seen in the RBS spectra of Fig. 4 as being due to deposition of these elements from ground water on the walls of the inter-granular spaces along which fracture has taken place. This is confirmed in the results of Fig. 5 which shows an electron microprobe scan for Fe, Ca and Ti, obtained using an electron microprobe with a 1 μm probe to scan a 1 mm thick slice of 1592 FTPV cut normal to the patinated surface. Clearly the elements in question are concentrated in localised regions separated by distances of the same order as the α-quartz grains. Note the enhancement of Fe seen at the surface by PIXE and in the SIMS result of Dr. W.O. Hofer, who analysed a similar sample (Hofer, 1974), is associated with an increase in the frequency of Fe peaks.

It is thus concluded that patination is the result of iron being transported inwards by ground water percolation along grain boundaries. The patination rate is thus dependent on the number and geometry of the inter-granular spaces and the local chemical environment and will vary widely from sample to sample. This reinforces the statement of Rottländer (1975, 1976) that thickness of patination cannot be used for dating and further the behaviour of iron and other trace elements throws considerable doubt on attempts at chert and flint-sourcing based on trace element composition (see Sieveking et al. (1972) de Bruin et al. (1972), Luedtke (1978, 1979), Domanski and Wojtowicz-Natanson (1980), Ferguson (1980), Craddock et al. (1983)).
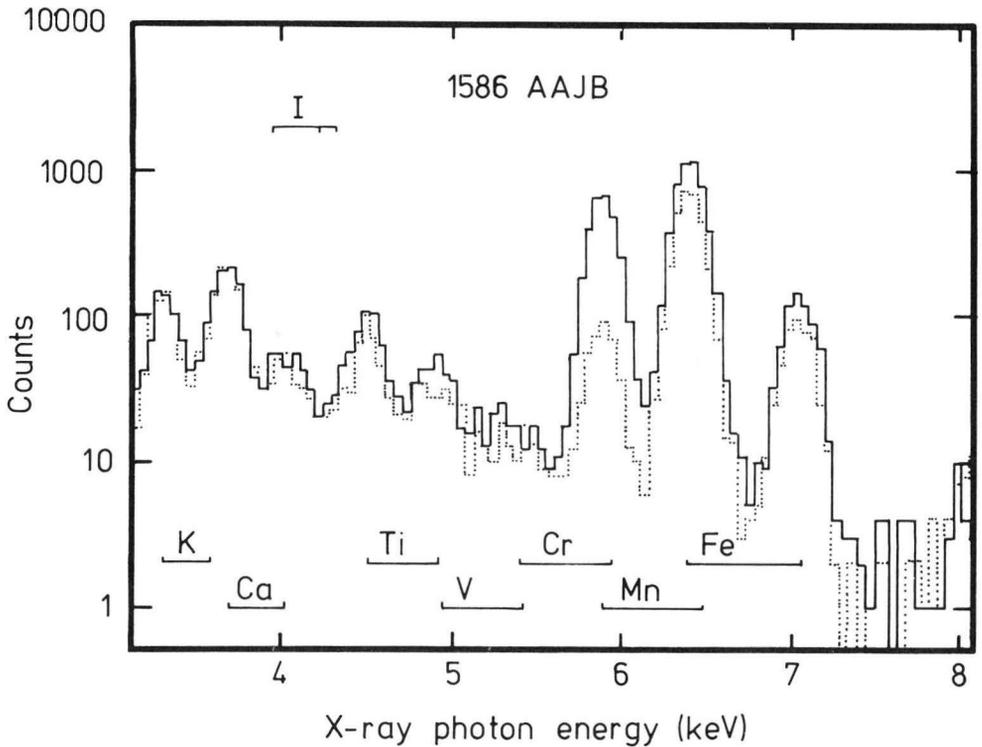
515

Fig. 6. PIXE spectra from 1586 AAJB. The solid line corresponds to the seaweed spot, the dotted line to a neutral surface. The Kα and Kβ line positions are shown for the various transition elements present. The (higher energy) Kβ line is 15 % the intensity of the Kα line. The iodine Lα, Lβ_1, Lβ_3 positions are also marked.

3.2 Seaweed spot patination

So-called »seaweed-spots» are patinated spots on the surface of flint of 0.5—2 cm diameter with brown to purple colouration. It was suspected that this colouration was due to deposition of iodine from holdfasts by which seaweed, a well known concentrator of iodine, attaches itself to rocks. In order to test this hypothesis we have investigated two archaeological samples and a modern flint sample from Moesgård beach on which seaweed *(fucus serratus)* was growing. The archaeological samples 1586 AAJB and 1586 HALP were from a mesolithic settlement at Brovst on Limfjorden in Northern Jutland (S.H. Andersen, 1969) which was covered by the sea approximately 4000 B.C. 1586 AAJB is a short, flat blade with brown spots of distinctly vegetable appearance on one surface. The spots on 1586 HALP which is a cleaver are of red/purple colouration. PIXE and RBS analysis showed that iodine was only present in significant quantities in the modern sample from which the seaweed had been dissected away. Fig. 6 shows a comparison of the PIXE spectra from the surface outside and inside a spot on 1586 AAJP; evidently the spot is associated with a higher Mn concentration. Quantitative analysis taking into account the interference between the Kα and Kβ lines of the adjacent elements shows the seaweed spot to be enhanced in Mn some 8 times over that of a neutral surface whilst Fe and V are enhanced by 2 times. Similar enhancements are seen for 1586 AAJB. Thus our seaweed spots are associated not with the presence of iodine but with enhanced transition-metal concentrations.
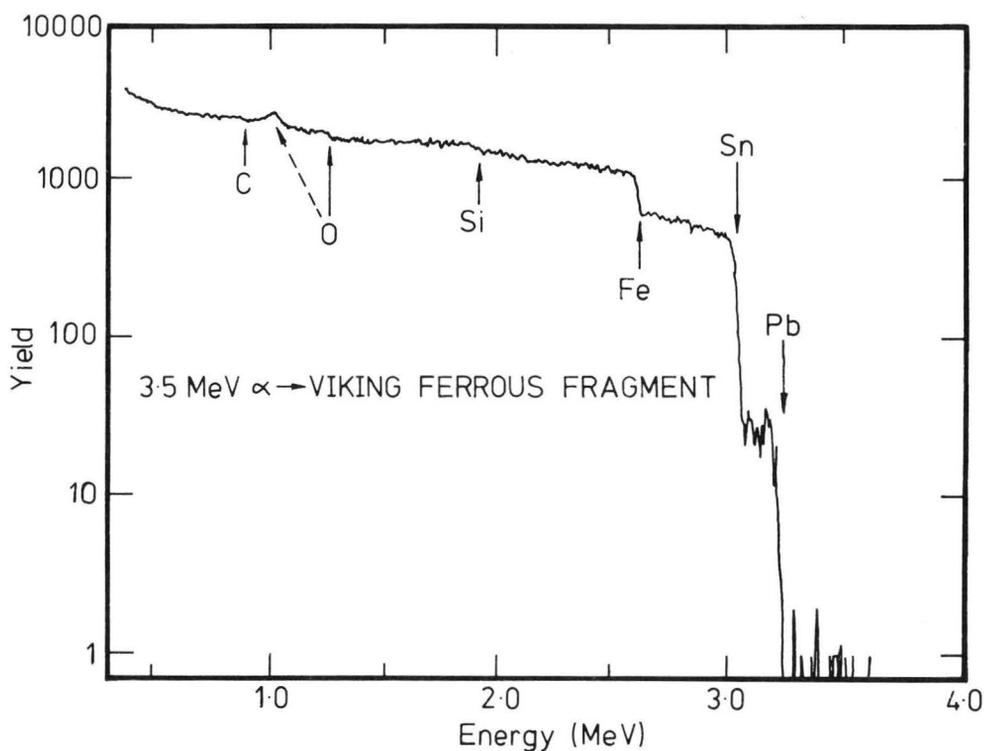
Fig. 7. RBS spectrum of the ferrous metal fragment in the »as-excavated» state.

(Transition metal compounds are often coloured.) In connection with this we note that the enhancement concentrations could be a consequence of deposition from marine organisms since in their body fluids the heavy element concentrations are often considerably greater than in the sea water of their environment.

3.3 Compositional analysis of ferrous metal fragment

Fig. 7 shows the RBS spectrum of a small fragment of an artefact found during excavation of a viking age settlement on the island of Fyn. The artefact which was some form of container was made out of ferrous metal and in a badly corroded state (Kelly 1981). We were interested in the metal joining technique used, which was suspected as being some form of soldering, and also if the chemical cleaning process used in conservation led to a change in composition of the artefact. For this purpose we were loaned two fragments of about 3 mm square taken from just below the edge of a reinforced rim. One fragment was in an »as-excavated» state whilst the other had been subjected to a proposed conservation technique in which the rust is removed by swabbing with ammonia solution. The RBS spectrum from the »as-excavated» sample (Fig. 7) shows contribution from Pb, Sn, Fe, Si, O and C. The Si, O and C are assumed to stem from soil adhering to the sample. The main components of the artefact are iron and tin which are homogeniously distributed within the outer 0.5 μm. The Sn/Fe composition ratio is about 25 at.%. Lead is present at the 0.5 at.% level. The presence of Pb and

517

Sn suggests that the artefact had been soldered. The artefact has a Pb/Sn concentration ratio of 2 at.% which is low in comparison with modern solders which contain 30—90 at.% Pb. It may be that »pure» tin was used as a solder in which Pb was present as a impurity or that Pb has been preferentially lost from a high-lead solder by corrosion. We note, however, that the Pb/Sn ratio is close to that of the protective coating on modern tin-plate which suggests the artefact may be of modern origin.

Comparison of the RBS spectra from the cleaned and uncleaned samples showed that the ammount of the contributions from oxygen and silicon were decreased by cleaning but no change occurred in the relative concentrations of Fe, Sn, and Pb, i.e. no change in artefact's composition was observed.

4. Conclusions

(i) The multi-elemental quantitative ion beam analysis by the PIXE and RBS techniques is well suited to determination of elemental compositions of artefacts. The larger sensitive depth of 5—10 μm for PIXE is better suited for study of macroscopic effects eg. colourations whilst the depth profiling capability of RBS makes it better suited for the study of archaeological and conservational processes concerned with the microstructure of artefacts.

(ii) The brown patination of flint is a consequence of the deposition of iron and other elements from groundwater salts onto the walls of the intergranular spaces and microfissures along which ground-water penetrates flint.

(iii) So-called seaweed spots on artefacts are associated with local enhancements of the Mn and other transition metal concentrations. These enhancements may be the result of the action of marine organisms.

(iv) RBS analysis of the metal fragment from a suspected viking age metal container showed this to be mainly Fe with 25 at.% Sn and 0.5 at.% Pb. This is consistent with the artefact being fabricated by soldering, however, the Pb/Sn ratio of 2 at.%, close to that of modern tin plate, suggests the artefact is of modern origin.

Acknowledgements

REFERENCES

Ahlberg, M., Akselsson, R., Forkman, B. and Rausing, G., 1976. Gold traces on wedge-shape artefacts from the late neolithic of southern Scandinavia analysed by proton induced X-ray spectrometry. Archaeometry 18, p. 39.
Ambrose, W.R., Duerden, P. and Bird, J.R., 1981. An archaeometric application of PIXE-PIGE to Admiralty Islands obsidians. Nucl. Instr. and Meth. 191, p. 397.
Andersen, H.H., 1982. A study of water uptake in flint. PACT, 7, p. 447.
Andersen, H.H. and Whitlow, H.J., 1983. Wear traces and patination on Danish flint artefacts. Nucl. Instr. and Meth. 218, p. 468.

Andersen, S.H., 1969. Brovst, en kystboplads fra ældre stenalder. KUML, Årb, f. Jysk Arkaeol. Selsk. 1969, p. 67.

Andersen, S.H., 1975. Ringkloster. En jysk indlandsboplads med Ærtebøllekultur. KUML Årb. f. Jysk Arkaeol.. Selsk. 1973—74, p. 11.

Baijot-Stroobands, I. and Bodart, F., 1977. Ancient pottery analysis by proton bombardment and Mössbauer spectroscopy. Nucl. Instr. and Meth. 142, p. 293.

Chen, H.-C., Chen, J.-X., Ren, C.-G., Xu, Z.-W., Yang, F.-C., Zhao, G.-Q. and Zhuo, Z.-Y., 1981. Ion beam analysis in Archaeology. Nucl. Instr. and Meth. 191, p. 391.

Chen, J.-X., Li, H.-K., Ren, C.-G., Tang, G.-H., Wang, X.-D., Yang, F.C. and Yao, H.-Y., 1980. PIXE research with an external beam. Nucl. Instr. and Meth. 168, p. 437.

Chu, W.K., Mayer, J.W. and Nicolet, M.-A., 1978. Backscattering Spectrometry, Academic Press.

Craddock, P.T., Cowell, M.R., Leese, M.N. and Hughes, M.J., 1983. The trace element composition of polished flint axes as an indicator of sources. Archaeometry 25, p. 135.

De Bruin, M., Korthoven, P.J.M., Bakels, C.C. and Groen, F.C.A., 1972. The use of non-destructive activation analysis and pattern recognition in the study of flint artefacts. Archaeometry 14, p. 55.

DeMortier, G. and Hackens, T., 1982. Milliprobe and microprobe analysis of gold items of ancient jewelry. Nucl. Instr. and Meth. 197, p. 223.

Domański, M. and Wojtowixz-Natanson, B., 1980. A possible application of the SIMS method to determine the provenance of the archaeological objects. Nucl. Instr. and Meth. 168, p. 435.

Duerden, P., Bird, J.R., Scott, M.D., Clayton, E., Russell, L.H and Cohen, D.D., 1980. PIXE-PIGE studies of artefacts. Nucl. Instr. and Meth. 168, p. 447.

Ferguson, J., 1980. Application of data coding to the differentiation of British flint mine sites. J. Archaeol. Sci. 7, p. 277.

Folkmann, F., 1975. Analytical use of ion-induced x-rays. J. Phys. E: Scientific Instruments 8, p. 429.

Hofer, W.O., 1974. Private communication.

Hyvönen-Dabek, M., 1981. Proton induced prompt gamma ray emission for determination of light elements in human bone. J. of Radioanaly. Chem. 63, p. 367.

Hänninen, R., Räisänen, J. and Anttila, A., 1980. Elemental analysis of Li and B with proton induced γ-ray reactions. Radiochem. Radioanal. Lett. 44, p. 201.

Johansson, S.A.E., Johansson, T.B., 1976. Analytical application of particle induced x-ray emission. Nucl. Instr. and Meth. 137, p. 473.

Kahn, Md.R., Crumpton, D., 1981. Proton induced x-ray emission analysis. CRC Critical Review in Analytical Chemistry 11, p. 104 and 11, p. 161.

Kelly, V., 1981. Private communication.

Luedtke, B.E., 1978. Chert sources and trace element analysis. American Antiquity 43, p. 413.

Luedtke, B.E., 1979. The identification of sources of chert artefacts. American Antiquity 44, p. 744.

Micheelsen, H., 1966. The structure of dark flint from Stevns, Denmark. Meddelelser fra Dansk Geologisk Forening Vol. 16, No. 3, p. 285.

Olausson, D.S. and Larsen, L., 1981. Heat treatment of flint in the scandinavian stone age. Meddelanden från Lunds Universitets historiska museum 1981—1982 (Papers of the Archaeological Institute University of Lund 1981—1982) New series Vol. 4. see also:

Olausson, D.S. and Larsson, L., 1982. Testing for the presence of thermal pretreatment of flint in the mesolithic and neolithic of Sweden. Journal of Archaeological Science 9, p. 275.

Rottländer, R., 1975. The formation of patination on flint. Archaeometry 17, p. 106.

Rottländer, R., 1976. Some aspects of the patination of flint. In, Engelen F. (ed.) Second Int. Symp. on Flint. Staringia No. 3, p. 54.

Räisänen, J., 1984. An external proton beam for PIGE analysis. Nucl. Instr. and Meth. B3, p. 220.

Saleh, N., Carlsson, L.-E., Hallk, A.B. and Bennet, C., 1981. PIXE analysis of ancient Jordanian pottery. Nucl. Instr. and Meth. 181, p. 527.

Sieveking, G., Craddock, P.T., Hughes, M.J., Bush, P.R. and Ferguson, I., 1970. Characterization of flint mine products. Nature, 228, p. 251.

Sieveking, G., Bush, P., Ferguson, I., Craddock, P.T., Hughes, M.J. and Cowell, M.R., 1972. Prehistoric flint mines and their identification as sources of flint material. Archaeometry 14, p. 151.